

Adaptive Mesh Segmentation for Modelling Dynamic Delamination Initiation and Propagation in Thick Composite Laminates

Jagan Selvaraj¹, Luiz Kawashita¹, Giuliano Allegri¹, Stephen Hallett¹

¹Bristol Composite Institute (ACCIS), University of Bristol, Queens Building, University Walk, Bristol BS8 1TR, UK

Abstract

Composites subjected to out-of-plane stresses due to impact loading can suffer from multiple delaminations, but modelling these in large scale structures is a challenging problem. To address this, a methodology is proposed for modelling dynamic delamination initiation and propagation in composites. It adaptively segments the mesh with additional nodes which model the discontinuities in the displacement field caused by delamination. Besides, it also introduces cohesive segments between the newly created nodes so that delamination propagation is controlled by an energy criterion. These adaptations are performed 'on-the-fly' in a dynamic explicit Finite Element solution without the need for user intervention, and the mesh segmentation technique does not reduce the time increment size for solution stability. A technique to initialise cohesive tractions with minimal disturbances to the surrounding stress field is also presented. This methodology is described here in detail and demonstrated in the commercial finite element software LS-Dyna. Finally, it is validated against experimental data from the existing literature.

1 Introduction

Different strategies for modelling the discontinuity which results from fracture have been developed over recent years. The concept of minimal remeshing has been tried by various authors with the addition of other features such as introduction of cohesive cracks [1], modelling of discontinuities using the phantom nodes, Phantom Node Method (PNM) [2] and the study of overlapping cohesive segments [3]. All the techniques vary in the choice of element formulation, type of solver and nature of the cohesive law.

The simplified cohesive segment method [4], presents the concept of minimal remeshing such that it can be applied easily via commercial solvers and it was originally developed for matrix cracking by splitting the elements.

In order to have the capability of initiating multiple delamination paths in thick composite laminates, a simple technique to model the displacement discontinuity is required. This technique should be efficient enough to be applicable in full-size simulations of impact events involving aero-engine components. The current work is aimed at using solid elements to the laminate, either with ply-level or sub-laminate level discretisation with an explicit time integration.

This paper discusses the general method of Adaptive Mesh Segmentation along with novel approaches for solving known issues around the initiation of cohesive segments while the analysis is being performed, namely (i) the criterion to initiate cohesive segments, and (ii) the detailed mapping of stresses from bulk element to cohesive segments at the time of initiation.

The initiation of cohesive segments is equivalent to introduction of a step function, and any errors introduced when projecting (or re-mapping) field variables will cause sudden local force imbalances which in explicit solutions manifest themselves as high-frequency oscillations.

In the past, authors have proposed to smear these residuals over arbitrary numbers of cycles to avoid the oscillations caused by crack extension [5]. However, these methods aim at damping down these oscillations as opposed to minimising the residuals which generate these in the first place.

2 Adaptive Mesh Segmentation

This section describes the modelling of displacement discontinuities using Adaptive Mesh Segmentation (AMS), which is the framework used here to introduce cohesive behaviour within continuum meshes 'on-the-fly', according to physically-based criteria and without direct user intervention.

2.1 Segmentation Procedure

Consider the element configuration shown in Figure 1. Let u and u' denote the global and local displacement vectors respectively. Let t_s be the time at which segmentation is initiated. Before the segmentation, the total number of nodes remains the same as the initial configuration (at time $t = 0$). Let n be the total number of nodes in the initial configuration, i.e. the 'parent nodes'. The displacement vectors of the element can be obtained by scattering global vectors into the corresponding location of each new element vector, i.e.

$$\text{Global displacement vector} = [u_1, u_2, \dots, u_{12}]^T \quad t \leq t_s \quad (1)$$

$$\text{Displacement vector of Element 1} = [u'_1, u'_2, \dots, u'_8]^T \text{ or } [u_1, u_2, u_3, u_4, u_5, u_6, u_7, u_8]^T \quad (2)$$

$$\text{Displacement vector of Element 2} = [u'_1, u'_2, \dots, u'_8]^T \text{ or } [u_5, u_6, u_7, u_8, u_9, u_{10}, u_{11}, u_{12}]^T \quad (3)$$

At time $t > t_s$, in order to initiate the split new nodes are initiated ('segmentation nodes'). It should be noted that segmentation nodes are initiated only at the location of existing parent nodes. The segmentation can be performed in such a way that all elements in the mesh can be split relative to each other, but only along the boundaries of these elements.

This method gives the following advantages, namely:

- Since the crack does not pass through the element, the element volume (and hence its Courant critical time step) are not affected by cohesive segmentation;
- The stress mapping after the split from the parent element to the newly formed element containing cohesive segment is less complex with this approach and introduces smaller errors in the solution;
- Since the crack does not pass through the integration points of element, further complexity is avoided. The problem of orienting the crack path has been discussed by other authors [4].

Segmentation nodes, marked in red in Figure 2, are initiated upon reaching a 'segmentation initiation criterion'. This involves re-defining the local mass matrix and ensuring that the stress tensor is compatible with the surrounding stress field so that disturbances are minimised.

Segmentation nodes form a segmentation vector (i.e. a plane defined by four points), which together with the global displacement vector models the discontinuities in displacement. At $t > t_s$, the segmentation and global displacement vectors for the example shown in Figure 2 would be,

$$\text{Global displacement vector} = [u_1, u_2, \dots, u_{12}]^T; \quad (4)$$

$$\text{Segmentation vector} = [u_a, u_b, u_c, u_d]^T; \quad (5)$$

$$\text{Displacement vector of Element 1} = [u_1, u_2, u_3, u_4, u_5, u_6, u_7, u_8]^T; \quad (6)$$

$$\text{Displacement vector of Element 2} = [u_a, u_b, u_c, u_d, u_9, u_{10}, u_{11}, u_{12}]^T. \quad (7)$$

This framework is implemented in the commercial software LS-Dyna through a series of user-defined element subroutines. All parent nodes are updated by LS-Dyna using the internal force vector calculated by the user subroutine. The time integration for segmentation nodes, once they are initiated, are done completely within the user subroutine.

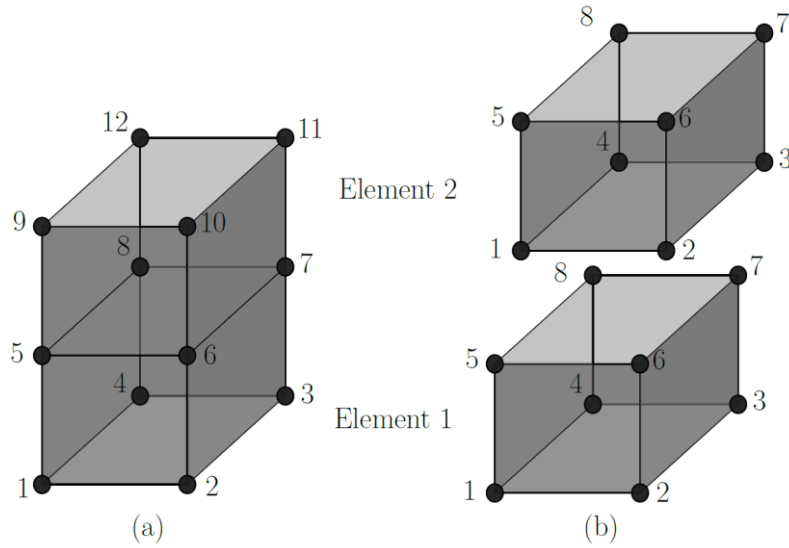


Fig. 1: Node numbering before segmentation ($t \leq t_s$); (a) global numbering and (b) local numbering. The scattering operation is based on equations (1)-(3)

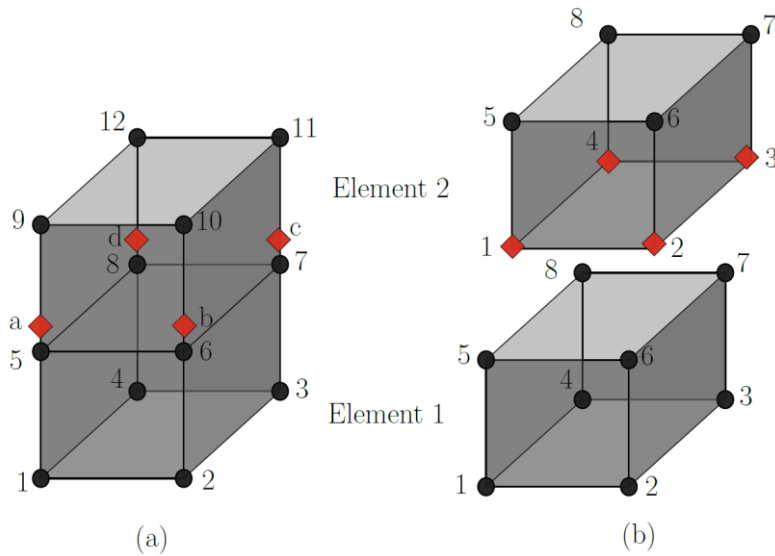


Fig. 2: Nodes after segmentation ($t > t_s$); (a) global numbering and (b) local numbering. The red rhombus represents the segmentation nodes. At the time of initiation, segmentation nodes are initiated from the location of parent nodes. The scattering operation is different from Figure 1 and is based on equations (4)-(7).

2.2 Segmentation Initiation Criterion

A simple approach to initiate cohesive segments is to use the quadratic damage initiation criterion. The tractions required in this criterion can be obtained from stresses in the bulk element. However, this approach results in considerable residuals primarily due to space discretisation errors and the lack of intra-element stress continuity in standard Finite Element solutions.

The proposed segmentation initiation criterion uses nodal forces and the area of cohesive segment to calculate the traction in the cohesive element. This traction will then be used to initiate cohesive segments with the exact cohesive tractions required to satisfy the momentum equation locally within the current time step.

Let f_1, f_2, f_3 be the nodal forces of each node in the bulk element obtained from internal force calculation (1,2 and 3 correspond to local direction).

The equivalent cohesive tractions can be calculated by using the forces in the bulk element by,

$$\tau_{33} = \frac{f_3}{A_{coh}}, \quad \tau_{23} = \frac{f_2}{A_{coh}}, \quad \text{and} \quad \tau_{13} = \frac{f_1}{A_{coh}} \quad (8)$$

where, A_{coh} is the area of the cohesive element per integration point. It is called equivalent cohesive traction to differentiate the cohesive traction obtained from cohesive element and the one used to check segmentation initiation.

The current work uses bilinear cohesive law developed at University of Bristol [6]. A history variable for damage is used such that the damage at a given time t , is the maximum value observed throughout the integration point's history.

Upon segmentation, cohesive integration points will have non-zero tractions. Physically, maximum traction across the crack surfaces must be achieved when the crack is initiated. To achieve this, the cohesive law is translated along the displacement direction such that the maximum traction is achieved for zero displacement across the crack surfaces [7]. However, mapping this traction is not a trivial problem, as discussed next in the section.

2.3 Errors Involved in the Initiation of Cohesive Segments

Consider a configuration where the cohesive segments are not initiated such that the discrete momentum equation is described only with parent nodes at time t . For all the nodes, n , in the domain Ω at time t ,

$$Ma^n = f^{ext} - f^{int} - f^{damp} \quad (9)$$

where f^{ext} , f^{int} and f^{damp} corresponds to external global force vector, internal global force vector and damping forces of the nodes. Since lumped mass matrix is used, the equations can be solved directly.

In the current problem, the boundary conditions are imposed as Dirichlet boundary conditions and no damping is given to the solver. So, the equation simplifies to,

$$Ma^n = -f^{int} \quad (10)$$

Before the crack is initiated, the sum of forces at the internal nodes will be zero such that $f^{int} = 0$. Let a_{new}^n be the acceleration of nodes that are initiated due to the formation of cohesive segments. At time $t + \Delta t$, cohesive segments are initiated such that the acceleration of the new nodes can be written as,

$$Ma_{new}^n = -f^{int} + f^{coh} \quad (11)$$

The segmentation error is defined as,

$$f^{error} = -f^{int} + f^{coh} \quad (12)$$

2.4 Initiation Based on Nodal Forces

The equation for cohesive force with $\tau_{initial}$ is given by,

$$f^{coh} = \int_{\xi} \int_{\eta} N^T \Phi^T \tau_{initial} J d\eta d\xi \quad (13)$$

$$A_{coh} = \int_{\xi} \int_{\eta} N^T \Phi^T J d\eta d\xi \quad (14)$$

where $\tau_{initial}$ represents the initial traction to be calculated using the proposed approach, N is the shape function matrix, Φ is the mapping from global to local coordinates and J is the area per integration point.

At the time of initiation, the nodal coordinates of cohesive segments are same as continuum element and it is possible to calculate A_{coh} . The internal nodal force vector corresponding to the location where additional nodes are inserted is $f_{initial}$.

Since we must get equal and opposite force to continuum element at the time of initiation, f^{coh} is replaced by $-f_{\text{initial}}$ in equation (11).

The required traction in the cohesive element is given by,

$$\tau_{\text{initial}} = -A_{\text{coh}}^{-1} f_{\text{initial}} \quad (15)$$

This traction is converted to displacement jump and passed to cohesive law. This method will give cohesive force that are equal and opposite to continuum element such that the error norm is zero.

Using penalty stiffness K and assuming that the integration point has not reached the initiation stress in cohesive law, τ_{initial} can be converted to displacement jump given by,

$$[[u]]^0 = \frac{1}{K} \tau_{\text{initial}} \quad (16)$$

Following the initiation, cohesive forces can be calculated. The time integration is performed for parent nodes and segmentation nodes using the nodal forces from bulk element and cohesive segment. This is where LS-Dyna Explicit solver and user defined solver work in parallel. All the parent nodes are solved by LS-Dyna whereas the segmentation nodes are solved with a user defined solver.

3 Results and Discussion

Benchmark cases are demonstrated using Double Cantilever Beam (DCB), End-Notch Flexure (ENF) and Fixed Ratio Mixed Mode (FRMM) specimens. The specimen dimensions and material properties are taken from the existing literature [8]. For all the cases present here, experimental results are available in the literature. However, only the analytical solution is compared to show the correlation in a clear way.

For all the cases shown here, mesh size of 0.25 mm was used. Even though the fracture process zone of different specimen varies, the mesh size was kept the same to get the close approximation of elastic stiffness. The time step for all the specimen was in the order of 10^{-6} s. The density of the material is in the order of 10^{-5} tonne/mm³. In all the benchmark cases shown, one element of size 0.25 mm was used in the width direction.

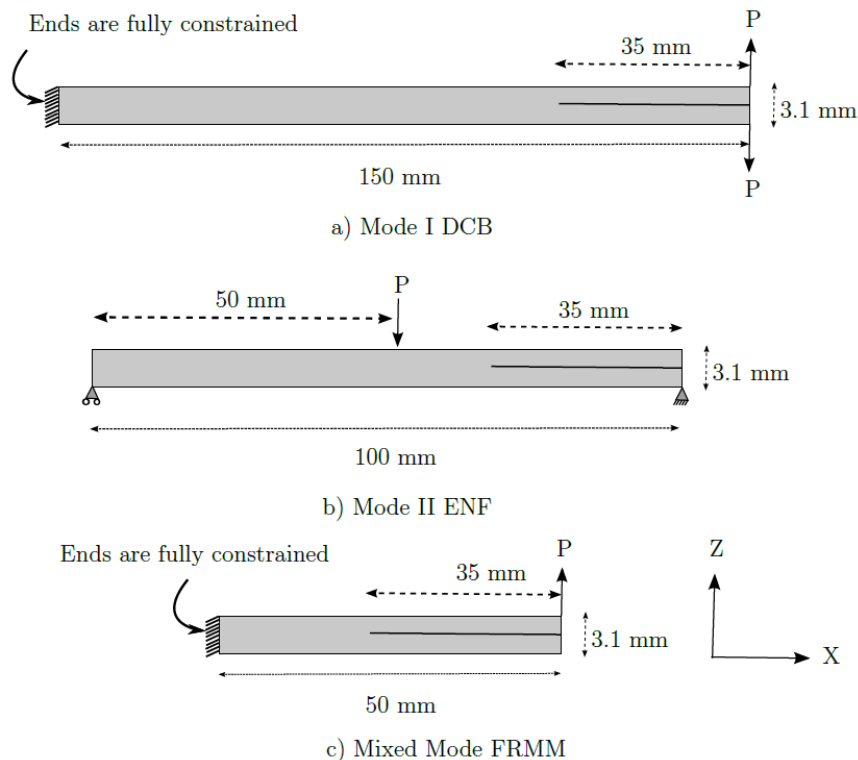


Fig.3: Dimensions of different specimens used to demonstrate segmentation

Table 1: Material parameters for HTA6376/C used in benchmark cases

E_{11} (GPa)	$E_{22} = E_{33}$ (GPa)	$G_{12} = G_{13}$ (GPa)	G_{23} (GPa)	$\nu_{12} = \nu_{13}$	ν_{23}
120	10.5	5.25	3.48	0.3	0.51
G_{Ic} (N/mm)	G_{IIc} (N/mm)	$\sigma_{I,max}$ (MPa)	$\sigma_{II,max}$ (MPa)	K_I N/mm ³	K_{II} N/mm ³
0.26	1.002	30.0	60.0	10 ⁵	10 ⁵

3.1 DCB

Stable initiation can be observed throughout the undamaged response portion of the load-displacement curve as shown in Fig 4. Damping is not given to the solver and it introduces oscillations in the damaged response. A good correlation can be seen during the initiation and propagation. In the absence of segmentation initiation criterion and initiation based on nodal forces, oscillations will manifest from the time segmentation is initiated.

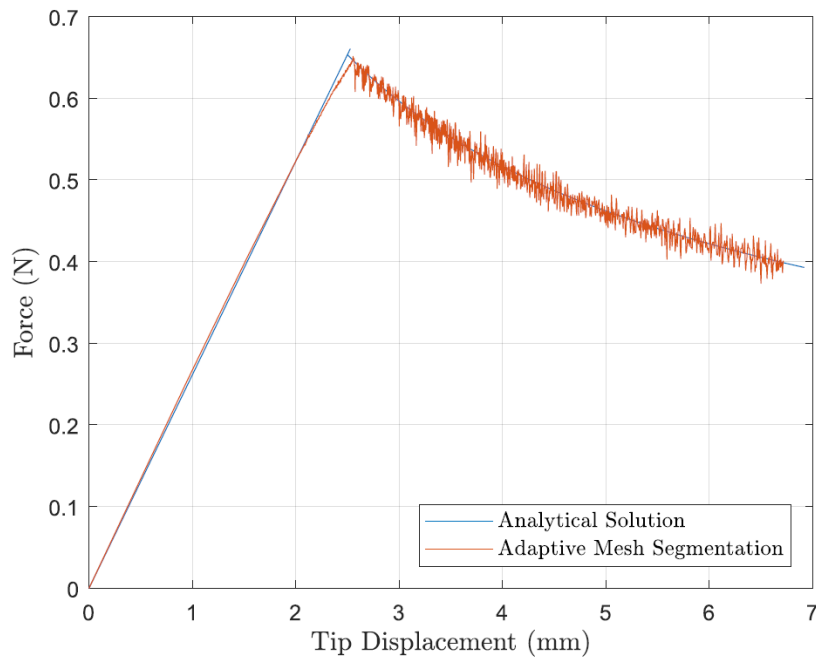


Fig.4: Comparison of DCB load-displacement curves obtained with AMS against analytic solution

3.2 ENF

ENF is one of the challenging tests to perform. The specimen includes the presence of point loads which induces compression and the initial split length of 35 mm must be resisted against penetration. The initial split length of 35 mm is also modelled with cohesive segments. The cohesive segments are used to resist the penetration.

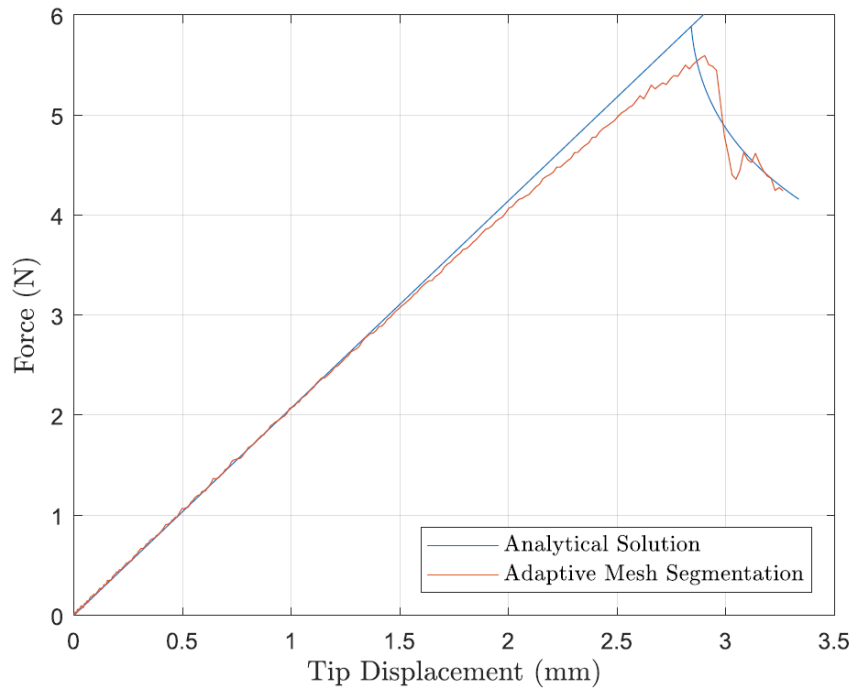


Fig.5: Comparison of ENF load-displacement curves obtained with AMS against analytic solution

3.3 FRMM

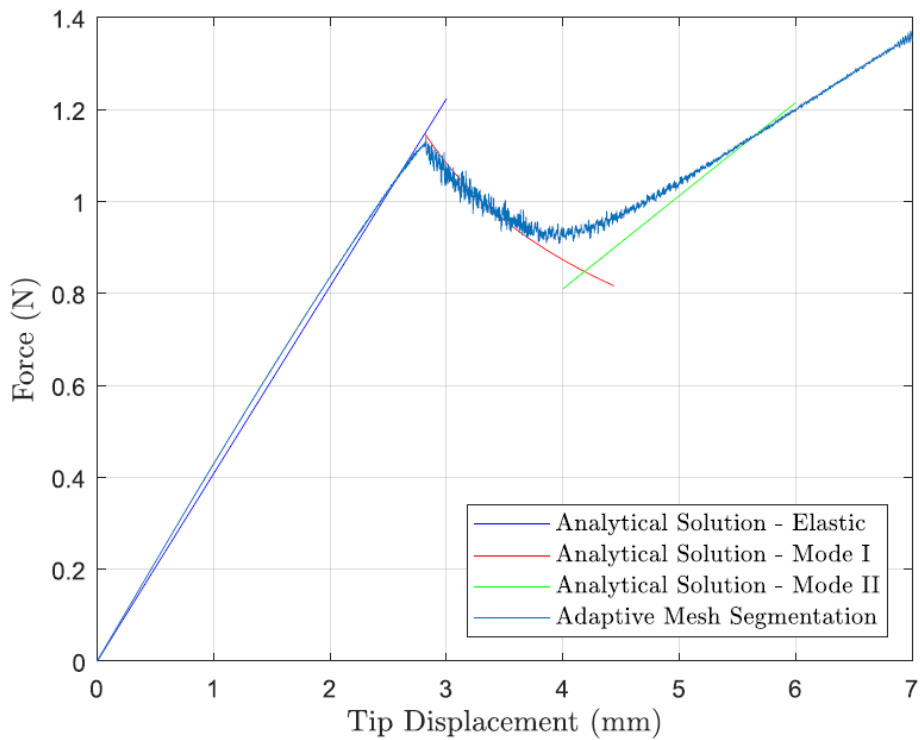


Fig.6: Comparison of FRMM load-displacement curves obtained with AMS against analytic solution

4 Conclusion

A method for adaptively segmenting the mesh locally to capture multiple delamination paths has been presented. It uses solid elements and explicit time integration. This method is being developed to handle loading cases such as impact and not just restricted to quasi static loading. So, the errors involved in initiating cohesive segments has been given requisite importance. If they are unchecked in benchmark cases presented here, the manifestation of errors will be high in extreme loading events. Also, Adaptive Mesh Segmentation is also implemented in commercial software LS-Dyna which allows the applicability of this method towards wider range of problems.

This method is specifically tailored to delamination as the crack path is restricted to element boundary. This restriction reduces the problem of stress mapping from bulk element to cohesive element. Also, stable time increment used in explicit analysis does not drop as the segmentation does not pass through the element.

Acknowledgements

This work was supported by Engineering and Physical Sciences Research Council through EPSRC centre for Doctoral training at the Bristol Composites Institute (ACCIS). Furthermore, the authors would like to acknowledge Rolls-Royce plc for their support of this research through Composites University Technology Centre at the University of Bristol, UK.

5 Literature

- [1] G. N. Wells and L. J. Sluys, "A new method for modelling cohesive cracks using finite elements," *Int. J. Numer. Methods Eng.*, vol. 50, no. 12, pp. 2667–2682, Apr. 2001.
- [2] J.-H. Song, P. M. A. Areias, and T. Belytschko, "A method for dynamic crack and shear band propagation with phantom nodes," *Int. J. Numer. Methods Eng.*, vol. 67, no. 6, pp. 868–893, Aug. 2006.
- [3] J. J. C. Remmers, R. de Borst, and A. Needleman, "A cohesive segments method for the simulation of crack growth," *Comput. Mech.*, vol. 31, no. 1–2, pp. 69–77, May 2003.
- [4] L. F. Kawashita, A. Bedos, and S. R. Hallett, "Modelling Mesh Independent Transverse Cracks in Laminated Composites with a Simplified Cohesive Segment Method," 2012.
- [5] T. Menouillard and T. Belytschko, "Smoothed nodal forces for improved dynamic crack propagation modeling in XFEM," *Int. J. Numer. Methods Eng.*, vol. 84, no. 1, pp. 47–72, Oct. 2010.
- [6] W.-G. Jiang, S. R. Hallett, B. G. Green, and M. R. Wisnom, "A concise interface constitutive law for analysis of delamination and splitting in composite materials and its application to scaled notched tensile specimens," *Int. J. Numer. Methods Eng.*, vol. 69, no. 9, pp. 1982–1995, Feb. 2007.
- [7] F. P. van der Meer, L. J. Sluys, S. R. Hallett, and M. R. Wisnom, "Computational modeling of complex failure mechanisms in laminates," *J. Compos. Mater.*, vol. 46, no. 5, pp. 603–623, Mar. 2012.
- [8] P. W. Harper and S. R. Hallett, "Cohesive zone length in numerical simulations of composite delamination," *Eng. Fract. Mech.*, vol. 75, no. 16, pp. 4774–4792, Nov. 2008.